ORIGINAL RESEARCH

Follow-Up of Coiled Cerebral Aneurysms at 3T: Comparison of 3D Time-of-Flight MR Angiography and Contrast-Enhanced MR Angiography

N. Anzalone
F. Scomazzoni
M. Cirillo
C. Righi
F. Simionato
M. Cadioli
A. Iadanza
M.A. Kirchin
G. Scotti

BACKGROUND AND PURPOSE: Our aim was to compare contrast-enhanced MR angiography (CE-MRA) and 3D time-of-flight (TOF) MRA at 3T for follow-up of coiled cerebral aneurysms.

MATERIALS AND METHODS: Fifty-two patients treated with Guglielmi detachable coils for 54 cerebral aneurysms were evaluated at 3T MRA. 3D TOF MRA (TR/TE = 23/3.5; SENSE factor = 2.5) and CE-MRA by using a 3D ultrafast gradient-echo sequence (TR/TE = 5.9/1.8; SENSE factor = 3) enhanced with 0.1-mmol/kg gadobenate dimeglumine were performed in the same session. Source images, 3D maximum intensity projection, 3D shaded surface display, and/or 3D volume-rendered reconstructions were evaluated in terms of aneurysm occlusion/patency and artifact presence.

RESULTS: In terms of clinical classification, the 2 MRA sequences were equivalent for 53 of the 54 treated aneurysms: 21 were considered fully occluded, whereas 16 were considered to have a residual neck and 16 were considered residually patent at follow-up MRA. The remaining aneurysm appeared fully occluded at TOF MRA but had a residual patent neck at CE-MRA. Visualization of residual aneurysm patency was significantly ($P = .001$) better with CE-MRA compared with TOF MRA for 10 (31.3%) of the 32 treated aneurysms considered residually patent with both sequences. Coil artifacts were present in 5 cases at TOF MRA but in none at CE-MRA. No relationship was apparent between the visualization of patency and either the size of the aneurysm or the interval between embolization and follow-up.

CONCLUSION: At follow-up MRA at 3T, unenhanced TOF and CE-MRA sequences are similarly effective at classifying coiled aneurysms as occluded or residually patent. However, CE-MRA is superior to TOF MRA for visualization of residual patency and is associated with fewer artifacts.

Regular imaging follow-up of patients with intracranial aneurysms treated with Guglielmi detachable coils (GDCs) is necessary because of the risk of aneurysm reconfiguration (ie, coil compaction and/or growth of a residual aneurysm neck or body remnant) with time.[1-4] Of the techniques available for monitoring the results of embolization therapy, MR angiography (MRA) has emerged as the technique of choice at most institutions. Advantages over conventional digital subtraction angiography (DSA) include minimal invasiveness with no associated risk of neurologic complications, reduced patient discomfort and inconvenience, greater cost savings, and no exposure to ionizing radiation or potentially nephrotoxic iodinated contrast media. An alternative minimally invasive procedure is CT angiography (CTA). However, whereas this technique has proved useful for aneurysm detection,[5-9] limitations to its use for follow-up of coiled aneurysms include streak and other coil-related artifacts.[10-12] Moreover, CTA also requires exposure to ionizing radiation and iodinated contrast media, which may be undesirable if repeat follow-up examinations are required.

Studies performed to date have shown that nonenhanced 3D time-of-flight (TOF) MRA sequences on 1.5T scanners are frequently satisfactory for the follow-up of coiled aneurysms[1-20] but that 3D TOF MRA on 3T scanners offers improved depiction of both treated[21] and untreated[22] aneurysms due to the greater spatial and contrast resolution achievable at a higher magnetic field strength. Concerning the use of gadolinium contrast material, some studies have suggested that contrast-enhanced MRA (CE-MRA) provides no additional benefit compared with nonenhanced 3D TOF MRA at either 1.5T[15,20] or 3T,[21] whereas other studies have shown that CE-MRA permits better visualization of coiled aneurysms and of branch arteries and residual neck, particularly in large or giant aneurysms.[14,22-26] Recently, Nael et al[27] demonstrated that CE-MRA with highly accelerated (×4) parallel acquisition at 3T provides comparable information to accelerated (×2) 3D TOF MRA at 3T for the characterization of untreated intracranial aneurysms without the known drawbacks of TOF MRA techniques (ie, prolonged acquisition time, spin saturation, and flow-related artifacts). On the other hand, Gibbs et al[28] showed that with elliptic-centric imaging, 3D TOF MRA at 3T is superior to CE-MRA at 3T in terms of both image quality and detection of untreated intracranial aneurysms. Our study was performed to evaluate CE-MRA with accelerated (×3) parallel acquisition at 3T compared with accelerated (×2.5) 3D TOF MRA at 3T for the follow-up of GDC-treated intracranial aneurysms. To the authors' knowledge, this is the first study to compare MRA sequences at 3T for follow-up of coiled aneurysms.

Materials and Methods

The study was a prospective evaluation of patients with GDC-treated intracranial aneurysms who were undergoing scheduled follow-up MRA as part of routine clinical practice. The study was approved by the local ethics review board. Because the study was conducted as part

Received February 21, 2008; accepted after revision April 11.

From the Department of Neuroradiology (N.A., F.S., M.C., C.R., F.S., M.C., A.I., G.S.), Ospedale San Raffaele, Milan, Italy; and Worldwide Medical and Regulatory Affairs (M.A.K.), Bracco Imaging SpA, Milan, Italy.

Please address correspondence to Nicoletta Anzalone, MD, Department of Neuroradiology, Scientific Institute, Ospedale San Raffaele, Milan, 20132, Italy; e-mail: anzalone.nicoletta@hsr.it

DOI 10.3174/ajnr.A1166

of routine practice and no additional invasive imaging was performed, written informed consent from evaluated patients was not required. Nevertheless, all patients were informed of the study, of its objectives, and of the potential clinical benefit the findings might reveal.

MR Imaging

MRA at 3T was performed on an Intera Scanner (Philips Medical Systems, Best, the Netherlands) by using a sensitivity-encoding (SENSE) head coil. Unenhanced 3D TOF MRA and CE-MRA were performed during the same imaging session in each patient. In all cases, 3D TOF MRA was performed first, followed by 3D CE-MRA. 3D TOF MRA was performed with TR = 23, TE = 3.5, FOV = 240, matrix = 240, and SENSE factor = 2.5. Data were acquired with a voxel size of $1 \times 1 \times 1$ mm, and images were reconstructed with a voxel size of $0.5 \times 0.5 \times 1$ mm through in-plane zero-filling interpolation. A total of 180 sections were obtained. The overall time for acquisition was 5 minutes 40 seconds. CE-MRA at 3T was performed by using a 3D section-interleaved gradient-echo sequence (TR = 5.9, TE = 1.8, flip angle = 40°, FOV = 220, matrix = 512, SENSE factor = 3) with 50% of overlap between sections. Data were acquired with a voxel size of $0.72 \times 0.72 \times 0.8$ mm, and images were reconstructed with a voxel size of $0.43 \times 0.43 \times 0.4$ mm through in-plane zero-filling interpolation. A total of 75 sections were acquired, and the overall time for acquisition was 24 seconds. CE-MRA images were acquired after administration of gadobenate dimeglumine (MultiHance; Bracco Imaging SpA, Milan, Italy) at a dose of 0.1 mmol/kg (0.2 mL/kg) bodyweight. Gadobenate dimeglumine was administered to all patients through an antecubital vein at a rate of 2 mL/s by using an MR imaging–compatible power injector (Spectris; MedRad, Indianola, Pa). All contrast administrations were followed by a 20-mL flush of 0.9% saline injected at the same rate of 2 mL/s.

Image Evaluation

The aim of the study was to compare 3D TOF MRA and CE-MRA at 3T for follow-up of cerebral aneurysms treated with GDCs. Image sets for each sequence and each patient comprised source images and 3D maximum-intensity-projection (MIP) reconstructions, 3D volume-rendered (VR) reconstructions, and 3D shaded surface display (SSD) reconstructions targeted on the vessel of interest. 3D TOF MRA and CE-MRA image sets were evaluated separately and independently in fully randomized order by 2 highly experienced readers in consensus. Treated aneurysms on each MRA image set were classified as described by Roy et al[29] as occluded or as demonstrating residual patency (type I aneurysm with residual neck or type II residual aneurysm).

Image sets were compared initially for differences in the visualization of embolization outcome (ie, occlusion versus residual neck versus residual aneurysm) and thereafter for the quality of visualization of residual patency. If treated aneurysms demonstrated residual patency on one or more image sets, the quality of visualization achieved by each sequence was graded by using a 3-point scale from −1 (sequence 1 better) through 0 (sequences equal) to +1 (sequence 2 better). A given MRA sequence was considered superior to the other on the basis of the quality of visualization of residual patency even if the clinical classification remained unchanged. Qualitative parameters taken into account in ascribing superiority included conspicuity of residual patency, size of residual patency, and contrast enhancement achieved. Artifactual signal-intensity loss in the region of the aneurysm was noted if present, but no cases were evaluated in which assessment of residual aneurysm patency was precluded by artifactual signal-intensity loss on either TOF MRA or CE-MRA. Superiority was only designated for tangible differences for which improved visualization might have clinical relevance.

Statistical Analysis

Comparison of the quality of the visualization of residual patency was performed by using the Wilcoxon signed rank test with a P value $<$ .005 considered statistically significant.

Results

Fifty-two patients (34 women, 18 men; mean age, 57.4 ± 9.8 years; range, 40–78 years) with a total of 54 cerebral aneurysms were evaluated. The interval between the follow-up MRA examination and the initial embolization was <6 months in 16 patients, between 6 months and 1 year in 7 patients, between 1 and 2 years in 12 patients, and ≥2 years in 17 patients. Thirty-five aneurysms were located in the internal carotid artery or carotid siphon; 11 were located in the anterior communicating artery; 7, in the vertebrobasilar system; and 1, in the middle cerebral artery. The 54 evaluated aneurysms were considered small (≤10 mm) in 43 cases (6.8 ± 1.8 mm), large (>10 mm, ≤25 mm) in 10 cases (14.4 ± 2.9 mm), and giant (>25 mm) in 1 case (26 mm).

Of the 54 treated aneurysms evaluated, 53 were classified equally with both sequences: 21 aneurysms were considered fully occluded, 16 were considered to have a residual neck, and 16 were considered residually patent with both sequences. A difference between TOF MRA and CE-MRA regarding the clinical classification of treated aneurysms was noted for just 1/54 (1.9%) aneurysms; this giant (26 mm) aneurysm was located at the apex of the right carotid siphon and appeared fully occluded on TOF MRA but with a residual neck on CE-MRA (Fig 1).

The visualization of residual patency was considered better after CE-MRA (on both MIP reconstructions and source images) compared with TOF MRA for the giant aneurysm and for 10 (6 small, 4 large; 31.3%) of the 32 treated aneurysms that demonstrated residual patency on both MRA sequences (Table). Conversely, visualization of residual patency was not superior on TOF MRA for any of the aneurysms. The number of aneurysms for which patency visualization was superior with CE-MRA was highly statistically significant (P = .001). Eight of these 10 aneurysms were located in the carotid system (5 small aneurysms, 3 large aneurysms) (Fig 2) with an additional 1 each in the anterior communicating artery (small) (Fig 3) and middle cerebral artery (large). In 8 (50%) cases, improved visualization on CE-MRA was noted for aneurysms considered residually patent (type II) (Fig 4), whereas in the remaining 2 (12.5%) cases (both small aneurysms), the better visualization was for treated aneurysms considered to have only a residual neck (Type I). Just 1 incompletely occluded aneurysm in the posterior communicating artery demonstrated a branch vessel arising from the sac. This was equally visible on both TOF and CE-MRA images.

There was no apparent time-related aspect to the visualization of residual patency. The 32 treated aneurysms considered residually patent or with residual neck on both MRA sequences comprised 7 in 7 patients undergoing follow-up MRA within 6 months of embolization, 7 in 7 patients undergoing

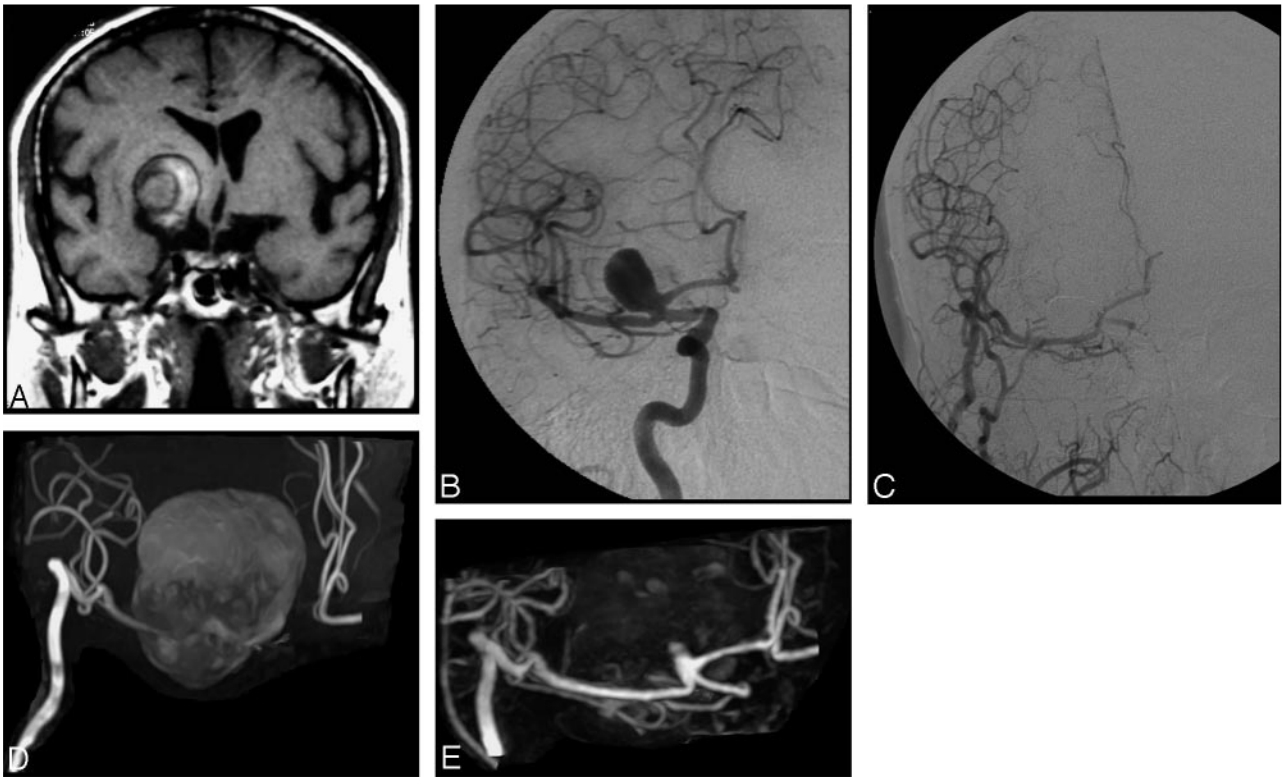

Fig 1. *A,* A large extra-axial lesion and hemorrhagic component indicative of a giant thrombosed aneurysm is apparent in the basal ganglia on the coronal T1-weighted MR image. *B,* Selective DSA of the right internal carotid artery before treatment reveals a patent portion of the giant thrombosed aneurysm. *C,* Selective DSA after embolization reveals complete occlusion of the aneurysm and a patent internal carotid artery–external carotid artery bypass. *D,* Follow-up 3D TOF MRA with MIP reconstruction performed at 1 year after treatment is inconclusive because of artifact related to the methemoglobin component of the thrombosed aneurysm. Additionally, flow-related signal intensity loss in the A1 segment of the anterior cerebral artery is apparent. *E,* Conversely, follow-up CE-MRA with MIP reconstruction demonstrates both the patent internal carotid artery–external carotid artery bypass and the presence of a small (type I) remnant at the neck of the treated aneurysm.

Comparison of TOF MRA with CE-MRA for visualization of residual aneurysm patency by the size of the treated aneurysm

Aneurysm Size	TOF MRA Better	Sequences Equal	CE-MRA Better
Small (n = 43)	0	37	6
Large (n = 10)	0	6	4
Giant (n = 1)	0	0	1
Total (n = 54)	0	43	11

Note:—TOF MRA indicates time-of-flight MR angiography; CE-MRA, contrast enhanced MR angiography.

follow-up MRA between 6 months and 1 year after embolization, and an additional 18 in 16 patients undergoing follow-up MRA at 1 year or more after embolization. Conversely, the aneurysms considered fully occluded on both sequences comprised 7 in 7 patients undergoing follow-up MRA within 6 months of embolization and 14 in 14 patients undergoing follow-up MRA at 1 year or more after embolization. The giant aneurysm that appeared occluded on TOF MRA but residually patent on CE-MRA was present in a patient who underwent follow-up imaging at 21 months after the embolization procedure.

A partial lack of signal intensity on TOF MRA image sets at the aneurysm site involving the parent artery or an adjacent vessel, which did not preclude evaluation of aneurysm patency, was noted for 5 small aneurysms (in 4 aneurysms in the left anterior communicating artery and in 1 at the right carotid siphon at the origin of the posterior communicating artery) and the single giant aneurysm (Fig 1*D*). These signal-intensity losses were not noted on the corresponding CE-MRA image sets and were considered primarily a result of saturation or susceptibility effects.

Discussion

Advantages of MR imaging with parallel imaging on higher magnetic field strength scanners lie in the greater spatial and temporal resolution achievable.[30-32] The greater spatial resolution on 3D TOF MRA at 3T has been shown to permit improved image quality and better visualization of small cerebral arteries[33] and better depiction of cerebrovascular disease, particularly intracranial aneurysms,[22,33] compared with 3D TOF MRA at 1.5T. A similar benefit for 3D TOF MRA at 3T has been shown for the follow-up of intracranial aneurysms after embolization with GDCs.[21] In this earlier study, Majoie et al[21] also acquired TOF MRA images at 3T after injection of contrast material (0.1-mmol/kg gadopentetate dimeglumine) but showed no additional benefit in terms of visualization of residual aneurysm remnants.

In contrast to the findings of Majoie et al,[21] our results suggest that image quality and the visualization of residual aneurysm patency on follow-up MRA at 3T can be improved still further if contrast enhancement is used with dedicated CE-MRA sequences in conjunction with parallel imaging. Specifically, significantly (P = .001) improved depiction of residual patency was observed on 3D CE-MRA in our study for 10/32 (31.3%) treated aneurysms that demonstrated residual patency also on 3D TOF MRA at 3T, whereas 1 giant an-

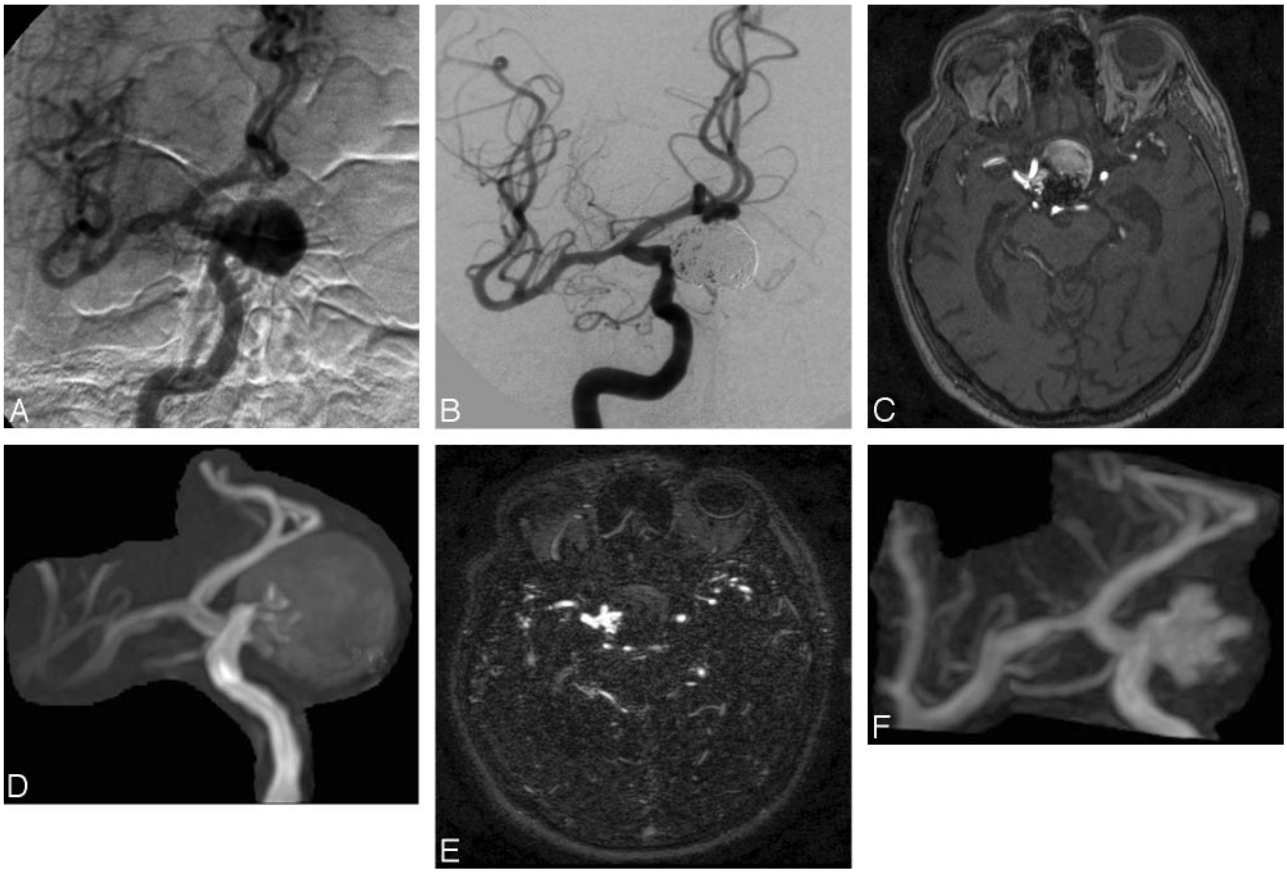

Fig 2. *A,* Selective DSA of the right internal carotid artery before treatment reveals a giant carotid-ophthalmic aneurysm. *B,* Selective DSA after embolization demonstrates complete occlusion of the aneurysm but with slightly reduced coil compaction near the neck. *C* and *D,* Follow-up 3D TOF MRA source image (*C*) and MIP reconstruction (*D*) obtained at 8 months after treatment reveal residual patency, but clear definition of the (type 2) remnant is compromised by saturation and methemoglobin artifact. *E* and *F,* Clearer depiction of the residual aneurysm is achieved on CE-MRA source images (*E*) and MIP reconstruction (*F*).

eurysm that appeared fully occluded on 3D TOF MRA at 3T was determined to have a residually patent neck at 3D CE-MRA at 3T. Notably, there was no case in which 3D TOF MRA at 3T was superior to 3D CE-MRA at 3T. Concerning the single giant aneurysm, the failure to demonstrate a residual neck on 3D TOF MRA was likely due to saturation effects, though flow-related signal intensity loss and methemoglobin T1 shinethrough effects cannot be excluded. The potential for spin saturation and signal-intensity loss associated with 3D TOF MRA sequences has been noted elsewhere as a potential drawback to follow-up imaging of giant aneurysms.[34] A similar loss of signal intensity on 3D TOF MRA image sets but not on 3D CE-MRA image sets was noted for 5 more aneurysms in addition to the solitary giant aneurysm and was considered primarily due to magnetic susceptibility effects as well as saturation effects arising from the location of these aneurysms. Each of these 5 aneurysms was small; this finding is consistent with that of other studies.[35]

Susceptibility effects are inherent in all metallic coil masses and may potentially obscure small neck remnants and adjacent structures, often resulting in a loss of signal intensity that is larger than the aneurysm itself. Potentially, the susceptibility effects at 3T are greater than those at 1.5T, despite the fact that the smaller voxel sizes achievable at 3T compared with 1.5T would tend to mitigate against greater susceptibility. In this regard, we recently showed no relevant differences in susceptibility for 3D TOF MRA acquisitions at 3T compared with 1.5T.[36] Another form of artifact inherent in the TOF MRA sequences is methemoglobin or "T1-shinethrough" effects resulting from subacute or chronic thrombus. Although methemoglobin effects can, in rare cases, obscure the hyperintensity of residual flow within the relevant vessels, the hyperintensity deriving from the thrombus is usually markedly less than that of the residually patent vessel or aneurysm.

Whereas susceptibility effects are a potential complication of unenhanced TOF sequences, theoretically, it is conceivable that residual hyperintensity in the neck of aneurysms on CE-MRA could be due to enhancing thrombus. However, this was not considered to be the case for any aneurysm in our series and, to our knowledge, has not yet been demonstrated or reported for similar patient series.

On the basis of aneurysm size alone, visualization of residual patency and branch arteries may be easier in the case of large or giant aneurysms than in the case of small aneurysms, particularly if the latter are located in anatomically unfavorable locations such as in the region of the anterior and posterior communicating arteries and basilar artery[19] or near the skull base where vessel overlap may interfere with evaluation of adjacent arterial vessels.[14] In our study, depiction of aneurysm patency with both MRA sequences was noted for 11/12 large aneurysms compared with 21/41 small aneurysms. The remaining large aneurysm and 20/41 small aneurysms were

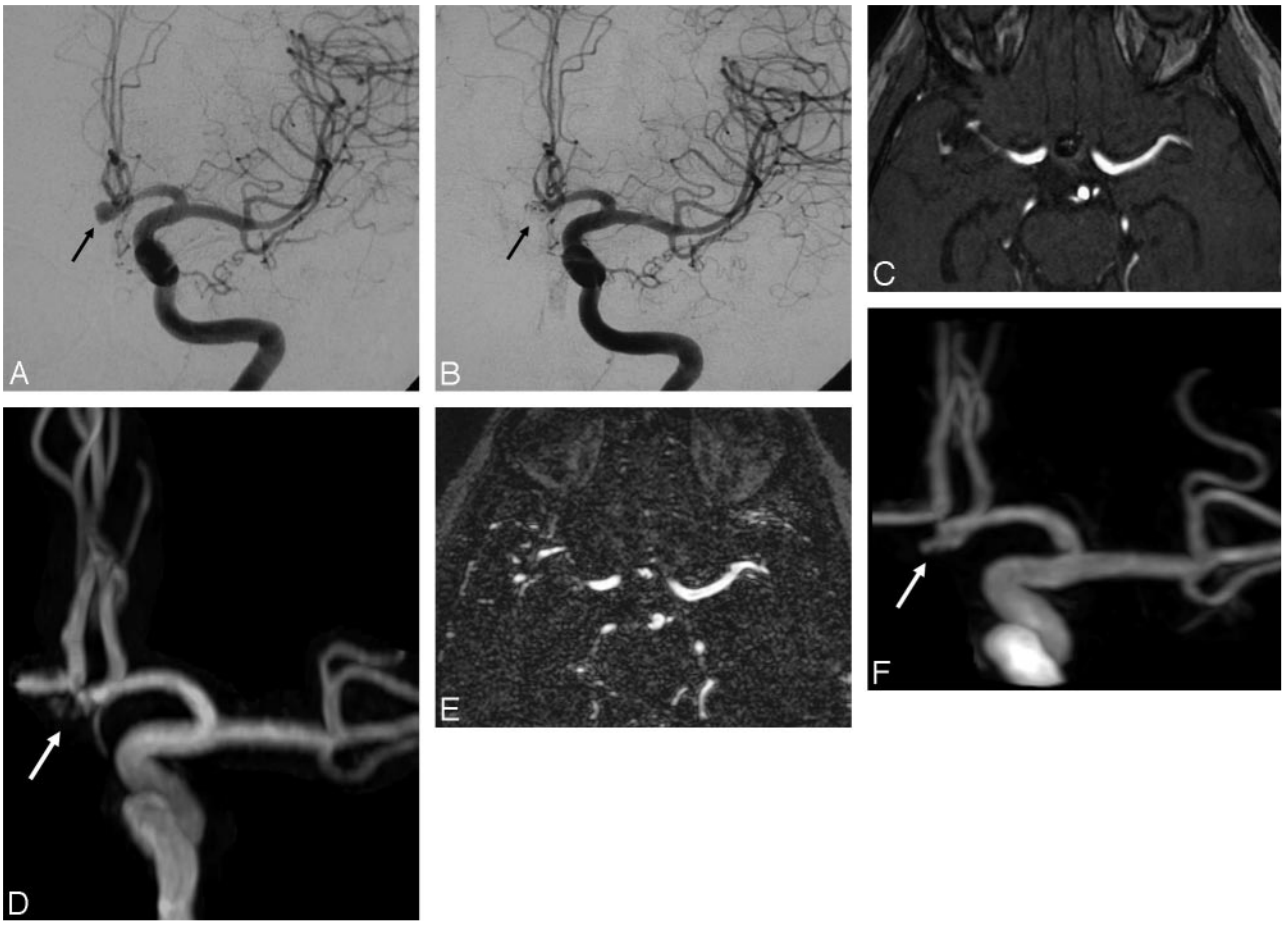

Fig 3. *A*, Selective DSA of the left internal carotid artery before treatment reveals a small aneurysm (*arrow*) of the anterior communicating artery. *B*, This aneurysm (*arrow*) appears completely occluded at follow-up DSA performed after embolization. *C* and *D*, Follow-up 3D TOF MRA source image (*C*) and MIP reconstruction (*D*) obtained at 3 months after treatment reveal high-signal-intensity inhomogeneities (arrow) in the region of the aneurysm neck but do not clearly demonstrate an aneurysm remnant. *E* and *F*, CE-MRA source image (*E*) and MIP reconstruction (*F*) clearly reveal the presence of a small (type 2) remnant.

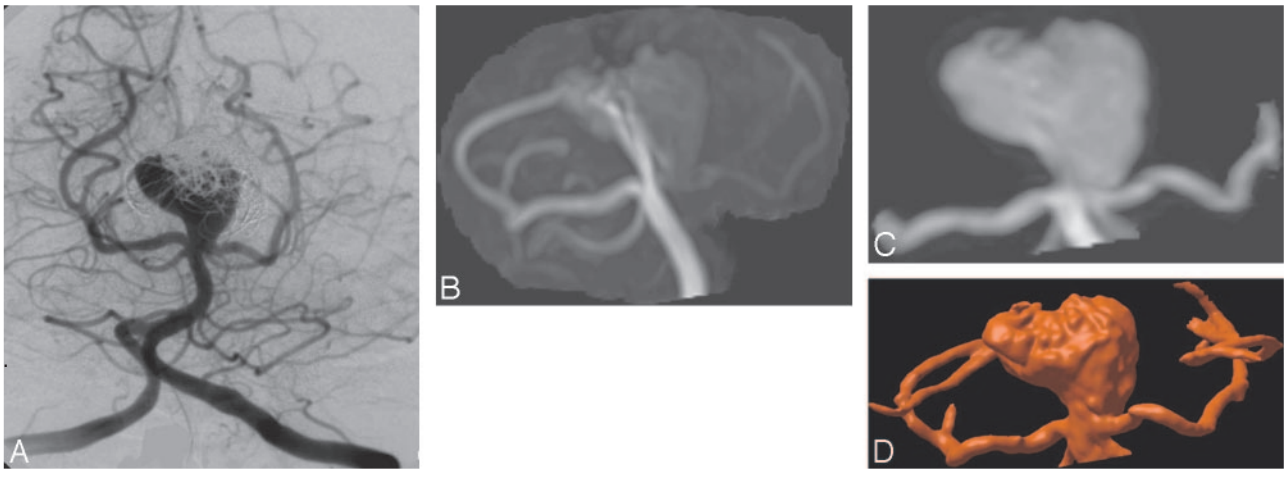

Fig 4. *A*, Follow-up DSA at 8 months after embolization of a large basilar artery aneurysm reveals only partial occlusion. *B*, 3D TOF MRA with MIP reconstruction (*B*) fails to show the (type 2) remnant entirely, due to flow effects that also compromise visualization of the left posterior cerebral artery. *C* and *D*, CE-MRA with MIP (*C*) and VR (*D*) reconstruction show both the artery and the residual aneurysm sac

considered fully occluded with both sequences. Notably, better definition of residual patency with CE-MRA was noted for 8 (50%) of 16 aneurysms considered type II for residual patency (ie, residual aneurysm) on both MRA sequences compared with only 2 (12.5%) of 16 aneurysms considered type I for residual patency (ie, residual neck).

A benefit of MR imaging at 3T compared with 1.5T is an increased baseline signal intensity-to-noise ratio (SNR) and hence improved vessel tissue contrast. However, the gain in signal intensity at 3T is largely offset by a loss of SNR when parallel image acquisition techniques are applied.[27,32,37] A standard means of maintaining adequate vessel tissue contrast

with parallel imaging techniques combined with dedicated CE-MRA sequences is to increase the SNR through the use of increased doses of gadolinium contrast material. Thus, Nael et al[27] administered a gadodiamide dose of 0.15 mmol/kg of bodyweight in their study, whereas Gibbs et al[28] administered 25 mL of gadoteridol, which corresponds to a total dose of approximately 0.15 mmol/kg of bodyweight for a person weighing 80 kg. In our study, an acceleration (SENSE) factor of ×3 was applied to the 3D CE-MRA acquisition. However, rather than use an increased dose of conventional gadolinium contrast agent, the potential loss of SNR was offset by the use of a standard 0.1-mmol/kg of bodyweight dose of gadobenate dimeglumine, a gadolinium agent with increased R1 relaxivity in blood[38,39] due to transient interaction with serum albumin.[40,41]

Numerous studies have demonstrated improved vascular imaging performance with gadobenate dimeglumine at a dose of 0.1 mmol/kg bodyweight compared with conventional gadolinium agents at equivalent or higher doses.[42-45] Although the use of gadolinium contrast agents does have certain potential disadvantages compared with unenhanced sequences (eg, cost, increased patient discomfort, complications of intravenous injections, and rare complications such as anaphylactoid reactions and nephrogenic systemic fibrosis), the possibility of obtaining greater qualitative information over that available on TOF MRA may nevertheless be of interest, particularly if the contrast agent used has proved advantages for vascular imaging and can be used at a reduced overall dose.

A possible limitation of our study is that no attempt was made to correlate findings on MRA at 3T with results from DSA. Numerous studies[13,14,16,18-26] as well as our own experience[36] have shown that MRA is a satisfactory noninvasive alternative to DSA for follow-up of aneurysms treated with GDCs, and as a result, DSA is no longer routinely performed at our center for this application.

Recently, the authors of a comprehensive review on the use of MRA for follow-up of coiled aneurysms stated that in their experience "3D TOF MRA without contrast is generally accurate and closely correlates with the findings of contrast-enhanced techniques" but that "in several cases contrast enhancement aided the visualization of small remnants and uncovered a larger neck remnant or filling of the coil pack that was not anticipated on the noncontrast MRA technique."[12] On the basis of their experience, they routinely perform CE-MRA along with 3D TOF MRA for the evaluation of coiled aneurysms. Our findings at 3T concur with this conclusion in showing that 3D CE-MRA at 3T is significantly better than 3D TOF MRA at 3T for the follow-up of coiled intracranial aneurysms.

Conclusion

At follow-up MRA at 3T unenhanced TOF and CE-MRA sequences are similarly effective at classifying coiled aneurysms as occluded or residually patent. However, CE-MRA is superior to TOF MRA for visualization of residual patency and is associated with fewer artifacts. Thus CE-MRA could be appropriate to better depict residual aneurysm patency even at 3T.

References

1. Cognard C, Weill A, Spelle L, et al. **Long-term angiographic follow-up of 169 intracranial berry aneurysms occluded with detachable coils.** *Radiology* 1999;212:348–56
2. Thornton J, Debrun GM, Aletich VA, et al. **Follow-up angiography of intracranial aneurysms treated with endovascular placement of Guglielmi detachable coils.** *Neurosurgery.* 2002;50:239–49
3. Raymond J, Guilbert F, Weill A, et al. **Long-term angiographic recurrences after selective endovascular treatment of aneurysms with detachable coils.** *Stroke* 2003;34:1398–403
4. Sluzewski M, van Rooij WJ, Slob MJ, et al. **Relation between aneurysm volume, packing, and compaction in 145 cerebral aneurysms treated with coils.** *Radiology* 2004;231:653–58
5. U-King-Im JM, Koo B, Trivedi RA, et al. **Current diagnostic approaches to subarachnoid haemorrhage.** *Eur Radiol* 2005;15:1135–47
6. Wintermark M, Uske A, Chalaron M, et al. **Multislice computerized tomography angiography in the evaluation of intracranial aneurysms: a comparison with intraarterial digital subtraction angiography.** *J Neurosurg* 2003;98:828–36
7. Kangasniemi M, Makela T, Koskinen S, et al. **Detection of intracranial aneurysms with two-dimensional and three-dimensional multislice helical computed tomographic angiography.** *Neurosurgery* 2004;54:336–40
8. Jayaraman MV, Mayo-Smith WW, Tung GA, et al. **Detection of intracranial aneurysms: multi-detector row CT angiography compared with DSA.** *Radiology* 2004;230:510–18
9. Hoh BL, Cheung AC, Rabinov JD, et al. **Results of a prospective protocol of computed tomographic angiography in place of catheter angiography as the only diagnostic and pretreatment planning study for cerebral aneurysms by a combined neurovascular team.** *Neurosurgery* 2004;54:1329–40
10. Korogi Y, Takahashi M, Katada K, et al. **Intracranial aneurysms: detection with three-dimensional CT angiography with volume rendering–comparison with conventional angiographic and surgical findings.** *Radiology* 1999;211:497–506
11. Masaryk AM, Frayne R, Unal O, et al. **Utility of CT angiography and MR angiography for the follow-up of experimental aneurysms treated with stents or Guglielmi detachable coils.** *AJNR Am J Neuroradiol* 2000;21:1523–31
12. Wallace RC, Karis JP, Partovi S, et al. **Noninvasive imaging of treated cerebral aneurysms. Part I: MR angiographic follow-up of coiled aneurysms.** *AJNR Am J Neuroradiol* 2007;28:1001–08
13. Kähärä VJ, Seppanen SK, Ryymin PS, et al. **MR angiography with three-dimensional time-of-flight and targeted maximum-intensity-projection reconstructions in the follow-up of intracranial aneurysms embolized with Guglielmi detachable coils.** *AJNR Am J Neuroradiol* 1999;20:1470–75
14. Anzalone N, Righi C, Simionato F, et al. **Three-dimensional time-of-flight MR angiography in the evaluation of intracranial aneurysms treated with Guglielmi detachable coils.** *AJNR Am J Neuroradiol* 2000;21:746–52
15. Cottier JP, Bleuzen-Couthon A, Gallas S, et al. **Intracranial aneurysms treated with Guglielmi detachable coils: is contrast material necessary in the follow-up with 3D time-of-flight MR angiography?** *AJNR Am J Neuroradiol* 2003;24:1797–803
16. Derdeyn CP, Graves VB, Turski PA, et al. **MR angiography of saccular aneurysms after treatment with Guglielmi detachable coils: preliminary experience.** *AJNR Am J Neuroradiol* 1997;18:279–86
17. Gönner F, Heid O, Remonda L, et al. **MR angiography with ultrashort echo time in cerebral aneurysms treated with Guglielmi detachable coils.** *AJNR Am J Neuroradiol* 1998;19:1324–28
18. Yamada N, Hayashi K, Murao K, et al. **Time-of-flight MR angiography targeted to coiled intracranial aneurysms is more sensitive to residual flow than is digital subtraction angiography.** *AJNR Am J Neuroradiol* 2004;25:1154–57
19. Deutschmann HA, Augustin M, Simbrunner J, et al. **Diagnostic accuracy of 3D time-of-flight MR angiography compared with digital subtraction angiography for follow-up of coiled intracranial aneurysms: influence of aneurysm size.** *AJNR Am J Neuroradiol* 2007;28:628–34
20. Pierot L, Delcourt C, Bouquigny F, et al. **Follow-up of intracranial aneurysms selectively treated with coils: prospective evaluation of contrast-enhanced MR angiography.** *AJNR Am J Neuroradiol* 2006;27:744–49
21. Majoie CB, Sprengers ME, van Rooij WJ, et al. **MR angiography at 3T versus digital subtraction angiography in the follow-up of intracranial aneurysms treated with detachable coils.** *AJNR Am J Neuroradiol* 2005;26:1349–56
22. Gibbs GF, Huston J 3rd, Bernstein MA, et al. **Improved image quality of intracranial aneurysms: 3.0-T versus 1.5-T time-of-flight MR angiography.** *AJNR Am J Neuroradiol* 2004;25:84–87
23. Boulin A, Pierot L. **Follow-up of intracranial aneurysms treated with detachable coils: comparison of gadolinium-enhanced 3D time-of-flight MR angiography and digital subtraction angiography.** *Radiology* 2001;219:108–13
24. Leclerc X, Navez JF, Gauvrit JY, et al. **Aneurysms of the anterior communicating artery treated with Guglielmi detachable coils: follow-up with contrast-enhanced MR angiography.** *AJNR Am J Neuroradiol* 2002;23:1121–27
25. Gauvrit JY, Leclerc X, Pernodet M, et al. **Intracranial aneurysms treated with**

Guglielmi detachable coils: usefulness of 6-month imaging follow-up with contrast-enhanced MR angiography. *AJNR Am J Neuroradiol* 2005;26:515–21
26. Farb RI, Nag S, Scott JN, et al. **Surveillance of intracranial aneurysms treated with detachable coils: a comparison of MRA techniques.** *Neuroradiology* 2005;47:507–15
27. Nael K, Villablanca JP, Saleh R, et al. **Contrast-enhanced MR angiography at 3T in the evaluation of intracranial aneurysms: a comparison with time-of-flight MR angiography.** *AJNR Am J Neuroradiol* 2006;27:2118–21
28. Gibbs GF, Huston J 3rd, Bernstein MA, et al. **3.0-Tesla MR angiography of intracranial aneurysms: comparison of time-of-flight and contrast-enhanced techniques.** *J Magn Reson Imaging* 2005;21:97–102
29. Roy D, Milot G, Raymond J. **Endovascular treatment of unruptured aneurysms.** *Stroke* 2001;32:1998–2004
30. Runge VM, Case RS, Sonnier HL. **Advances in clinical 3-Tesla neuroimaging.** *Invest Radiol* 2006;41:63–67
31. Willinek WA, Kuhl CK. **3.0 T neuroimaging: technical considerations and clinical applications.** *Neuroimaging Clin N Am* 2006;16:217–28, ix
32. Nael K, Michaely HJ, Villablanca P, et al. **Time-resolved contrast enhanced magnetic resonance angiography of the head and neck at 3.0 Tesla: initial results.** *Invest Radiol* 2006;41:116–24
33. Willinek WA, Born M, Simon B, et al. **Time-of-flight MR angiography: comparison of 3.0-T imaging and 1.5-T imaging—initial experience.** *Radiology* 2003;229:913–20
34. Thomas B, Sunaert S, Thamburaj K, et al. **Spurious absence of signal on 3D time-of-flight MR angiograms on 1 and 3 Tesla magnets in cerebral arteries associated with a giant ophthalmic segment aneurysm: the need for alternative techniques.** *JBR-BTR* 2005;88:241–44
35. Schuierer G, Huk WJ, Laub G. **Magnetic resonance angiography of intracranial aneurysms: comparison with intra-arterial digital subtraction angiography.** *Neuroradiology* 1992;35:50–54
36. Anzalone N, Scomazzoni F, Cirillo M, et al. **Follow-up of coiled cerebral aneurysms: comparison of 3D TOF-MRA at 3 Tesla with 3D TOF-MRA and contrast-enhanced MRA at 1.5 Tesla.** *Invest Radiol* 2008;43:559–67
37. Nael K, Ruehm SG, Michaely HJ, et al. **High spatial-resolution CE-MRA of the carotid circulation with parallel imaging: comparison of image quality between 2 different acceleration factors at 3.0 Tesla.** *Invest Radiol* 2006;41:391–99
38. Pintaske J, Martirosian P, Graf H, et al. **Relaxivity of gadopentetate dimeglumine (Magnevist), gadobutrol (Gadovist), and gadobenate dimeglumine (MultiHance) in human blood plasma at 0.2, 1.5, and 3 Tesla.** *Invest Radiol* 2006;41:213–21
39. Rohrer M, Bauer H, Mintorovitch J, et al. **Comparison of magnetic properties of MRI contrast media solutions at different magnetic field strengths.** *Invest Radiol* 2005;40:715–24
40. Cavagna FM, Maggioni F, Castelli PM, et al. **Gadolinium chelates with weak binding to serum proteins: a new class of high-efficiency, general purpose contrast agents for magnetic resonance imaging.** *Invest Radiol* 1997;32:780–96
41. Giesel FL, von Tengg-Kobligk H, Wilkinson ID, et al. **Influence of human serum albumin on longitudinal and transverse relaxation rates (R1 and R2) of magnetic resonance contrast agents.** *Invest Radiol* 2006;41:222–28
42. Knopp MV, Schoenberg SO, Rehm C, et al. **Assessment of gadobenate dimeglumine (Gd-BOPTA) for MR angiography: phase I studies.** *Invest Radiol* 2002;37:706–15
43. Knopp MV, Giesel FL, von Tengg-Kobligk H, et al. **Contrast-enhanced MR angiography of the run-off vasculature: intraindividual comparison of gadobenate dimeglumine with gadopentetate dimeglumine.** *J Magn Reson Imaging* 2003;17:694–702
44. Pediconi F, Fraioli F, Catalano C, et al. **Gadobenate dimeglumine (Gd-BOPTA) vs gadopentetate dimeglumine (Gd-DTPA) for contrast-enhanced magnetic resonance angiography (MRA): improvement in intravascular signal intensity and contrast to noise ratio** [in English and Italian]. *Radiol Med (Torino)* 2003;106:87–93
45. Prokop M, Schneider G, Vanzulli A, et al. **Contrast-enhanced MR angiography of the renal arteries: blinded multicenter crossover comparison of gadobenate dimeglumine and gadopentetate dimeglumine.** *Radiology* 2005;234:399–408. Epub 2004 Dec 22